

Clusters in the DISPERSE cosmic web

J.D. Cohn^{1,2*}

¹*Space Sciences Laboratory University of California, Berkeley, CA 94720, USA*

²*Theoretical Astrophysics Center, University of California, Berkeley, CA 94720, USA*

30 March 2022

ABSTRACT

Galaxy cluster mass halos (“clusters”) in a dark matter simulation are matched to nodes in several different cosmic webs found using the DISPERSE cosmic web finder. The webs have different simulation smoothings and DISPERSE parameter choices; for each, 4 methods are considered for matching DISPERSE nodes to clusters. For most of the webs, DISPERSE nodes outnumber clusters, but not every cluster has a DISPERSE node match (and sometimes > 1 cluster matches to the same DISPERSE node). The clusters frequently lacking a matching DISPERSE node have a different distribution of local shear trends and perhaps merger histories. It might be interesting to see in what other ways, e.g., observational properties, these clusters differ. For the webs with smoothing $\leq 2.5 Mpc/h$, and all but the most restrictive matching criterion, $\sim 3/4$ of the clusters always have a DISPERSE node counterpart. The nearest cluster to a given DISPERSE node and vice versa, within twice the smoothing length, obey a cluster mass-DISPERSE node density relation. Cluster pairs where both clusters match DISPERSE nodes can also be assigned the filaments between those nodes, but as the web and matching methods are varied, most such filaments do not remain. There is an enhancement of subhalo counts and halo mass between cluster pairs, averaging over cluster pairs assigned DISPERSE filaments increases the enhancement. The approach here also lends itself to comparing nodes across many cosmic web constructions, using the fixed underlying cluster distribution to make a correspondence.

Key words: cosmology:large scale structure of the Universe, galaxies:clusters

The cosmic web (Bond, Kofman & Pogosyan 1996; Bond & Myers 1996; Pogosyan, Bond & Kofman 1998) exists within many tracers of large scale structure in the universe, from galaxies to dark matter to gas, and underpins the evolution of large scale structure. In the many years since its discovery, numerous ways of characterizing the web and identifying its components (nodes, filaments, voids and walls) have been proposed. Several of these web finders are compared in Libeskind et al (2018), earlier comparisons include, e.g., Leclercq et al (2016); see also the recent meetings (van de Weygaert et al 2016; Higgs Cosmic Web 2019).

In large scale structure, galaxy cluster mass halos (“clusters” henceforth) are the most massive bound structures; often clusters are referred to as nodes in the cosmic web. This correspondence frequently holds: in the web finder comparison of Libeskind et al (2018), most of the clusters lie in cosmic web nodes in all definitions considered. Properties of the relation between clusters and different variants of the web have been studied for a long time, for instance in the context of the peak-patch algorithm (Bond & Myers 1996), or using the Gaussian field methods of Bardeen et al (1986), also see the review of van de Weygaert & Bond (2008). Clusters have also been used to infer initial conditions, which are then run for-

ward in time to get large scale properties including the cosmic web (e.g., Bos et al 2016; Bos 2016).

In this note, cluster-node correspondences and properties of filaments linking clusters are explored in more detail, for nodes and filaments in cosmic webs found via DISPERSE within a single dark matter simulation. The aim here is to see how nodes in these cosmic webs correspond to clusters, and from there, how the cluster pairs correspond to node pairs which are connected by filaments. The initial expectation was that the clusters would pick out special nodes in the cosmic web(s) and that the filaments would pick out special associated cluster pairs. However, for the webs and cluster-node matchings used here, not all clusters had a node counterpart. So in addition to clusters picking out certain nodes in the webs, the webs picked out certain clusters.

The underlying dark matter simulation and the web finder DISPERSE are described in §1, as well as a Hessian based node finder (used later as part of one matching method). In §2 a few methods to match clusters and DISPERSE nodes are suggested, applied and compared. Cluster pairs are matched to DISPERSE filaments in §3 and properties of cluster pairs with and without these filaments are explored in §4. §5 concludes.

* E-mail: jcohn@berkeley.edu

1 SIMULATION DATA AND WEB FINDERS

1.1 Simulation database

The dark matter density map and halo and subhalo samples are taken from the publicly available Millennium simulation (Springel et al 2005) and its database (Lemson & Springel 2006). The simulation corresponds to a fixed time box with side $500 Mpc/h$ and 2160^3 particles; redshift $z = 0.12$ (step 58) is used. The densities (relative to mean) are available in the simulation on a 256^3 pixel grid, with Gaussian smoothing radii of $1.25 Mpc/h$, $2.5 Mpc/h$, $5 Mpc/h$.¹ The commonly used $2 Mpc/h$ smoothing (e.g., Hahn et al 2007a,b) is included by further smoothing the $1.25 Mpc/h$ overdensities. The halos are found via Friends of Friends (FoF) (Davis et al 1985) with linking length 0.2, and the subhalos are found via SUBFIND (Springel et al 2005). Subhalos (considered in §4.2, §4.3) can be central, satellite or orphans; their virial mass is the mass of the FoF group they were in when they were last a central subhalo. The 2898 massive halos with $M_{\text{vir}} \geq 10^{14} M_{\odot}$ are taken to be clusters². The Planck cosmology (Planck collaboration 2018) Millennium simulation is created from the original Millennium simulation by shifts and scalings (Angulo & White 2010; Angulo & Hilbert 2015), however, the rescaled density field grid is unavailable. So the cosmological parameters are unfortunately outdated ($\Omega_m = 0.25$, $\Omega_b = 0.045$, $h = 0.73$, $n=1$, $\sigma_8 = 0.9$). However, the particular cosmology is likely irrelevant to the qualitative questions of interest here.

1.2 Finding the web

Many different web finders have been implemented and studied in past decades. The resulting different webs capture different physical aspects and are based upon a wide range of tracers (e.g., dark matter densities, galaxy positions, velocities, etc.) and algorithms, e.g., eigenvalues of the shear tensor (e.g., Zel'dovich 1970; Hahn et al 2007a,b), density critical points and the ridges connecting them e.g., DISPERSE (Sousbie 2011; Sousbie, Pichon, & Kawahara 2011), MMF-2 (Aragon-Calvo et al 2007), NEXUS (Cautun, van de Weygaert & Jones 2013), shell crossing histories and flows (Shandarin & Zel'dovich 1989; Shandarin 2011), phase space ORIGAMI (Falck, Neyrinck & Szalay 2012; Falck & Neyrinck 2015), MWSA (Ramachandra & Shandarin 2015), etc. In Libeskind et al (2018), twelve approaches were classified, reviewed, applied and compared. Using a common $200 Mpc/h$ side dark matter simulation, the webs resulting from the different approaches were compared via volume and mass fractions for each web component, overlaps between the same components with different finders, and more. Webs can

¹ For $1.25 Mpc/h$ smoothing, “select a.phkey, a.g1.25 from MField.MField as a where a.snapnum=58 order by a.phkey”. For larger smoothings, substitute $g2.5$ and $g.5$.

² Cluster mass halos are downloaded via “select a.galaxyId, a.phKey, a.mvir, a.x, a.y, a.z, a.type from MPAGalaxies.deLucia2006a as a where a.phKey between NNN and MMM and a.mvir >= 7300 and a.type=0 and a.snapnum=58”, where NNN, MMM select a phKey subset, and mvir is virial mass of the FoF subhalo. This is done for all phKeys by doing for several ranges of NNN, MMM.

also be characterized by node connectivity and angular dependence, studied, e.g., in Gaussian fields and simulations (Codis, Pichon, & Pogosyan 2018), via histories and mergers of critical points (Cautun et al 2014; Cadiou et al 2020), and in terms of their relations to many different galaxy properties (there is a very long list, see, e.g., Hellwing et al 2021; Winkel et al 2021). Since the Libeskind et al (2018) comparison paper, methods for web detection (Fang et al 2019; Pereyra et al 2020; Wang et al 2020) and web finder comparison methods (e.g., between filaments, Rost et al 2020) have continued to be developed. Each web finding method involves choices of parameters, scales and (sometimes implicitly) other assumptions.

The main web finder used here is DISPERSE (Sousbie 2011; Sousbie, Pichon, & Kawahara 2011)³, a publicly available code which does a multiscale identification of all 4 web components starting with individual objects (such as galaxies) or a density field. Here, the (Gaussian) smoothed density field is taken to be the starting point and DISPERSE is used to identify nodes and filaments from pixel maps of simulation densities relative to the mean.⁴ Using Morse theory, DISPERSE classifies regions using critical points (nulls of the gradient of the field) and integral lines (tangents to the field at every point, which converge at critical points). In addition to the underlying smoothing and pixel size, the DISPERSE web also depends on “persistence”, a parameter describing roughly how much a field has to decrease between two peaks in order for them to be considered as distinct peaks. As the persistence rises, DISPERSE nodes are removed. Persistence levels in the examples below are taken to be 1σ , 2σ and 3σ of the density field; although 1σ is a low persistence choice, it helps in examining trends with persistence.⁵

With the DISPERSE webs, the nodes are points (dimension zero)⁶ and the filaments are curves (dimension 1) associated with saddle critical points (dimension 0), none of which have associated volume. One way to associate clusters to a web node is to have the cluster lying “in” the node. Two obvious scales for assigning volume to DISPERSE nodes, within which a cluster could lie, are the pixel size and smoothing scale. A third way to associate volume to a DISPERSE node, which uses more information from the density field, is based upon the Hessian based web finder, or “T-web”; some recent descriptions are in Hahn et al (2007a,b). (Other ways of possibly defining the “width” of a DISPERSE node or filament, beyond what will be considered here, include stacking DISPERSE objects (Kraljic et al 2019) or looking at vorticity behavior (Laigle et al 2015).) To classify pixels in terms of cosmic web

³ <http://www2.iap.fr/users/sousbie/web/html/indexd41d.html>

⁴ The added level of complication for DISPERSE on subhalo counts became unmanageable in practice for the available computing resources and current data set.

⁵ To run, DISPERSE uses a file of pixel density values, e.g., “pixfile.dat”. One chooses persistence “pers”, which is a number, and runs `MSE PIXFILE.DAT -CUT PERS -UPSKL`. On that output, `up.NDskl` one runs `SKELCONV OUTPUT.UP.NDskl -OUTNAME PIXFILE -TO NDskl.LASCH` to get `pixfile.a.NDskl`, with node and saddle (filament center) critical points and information about each.

⁶ The allowed DISPERSE node positions on a pixel are at $(0, 1/4, 1/3, 1/2, 2/3, 3/4)$ in pixel units. The pixel size $500/256 Mpc/h$ is used to rescale, and then DISPERSE provided positions are shifted by half a pixel.

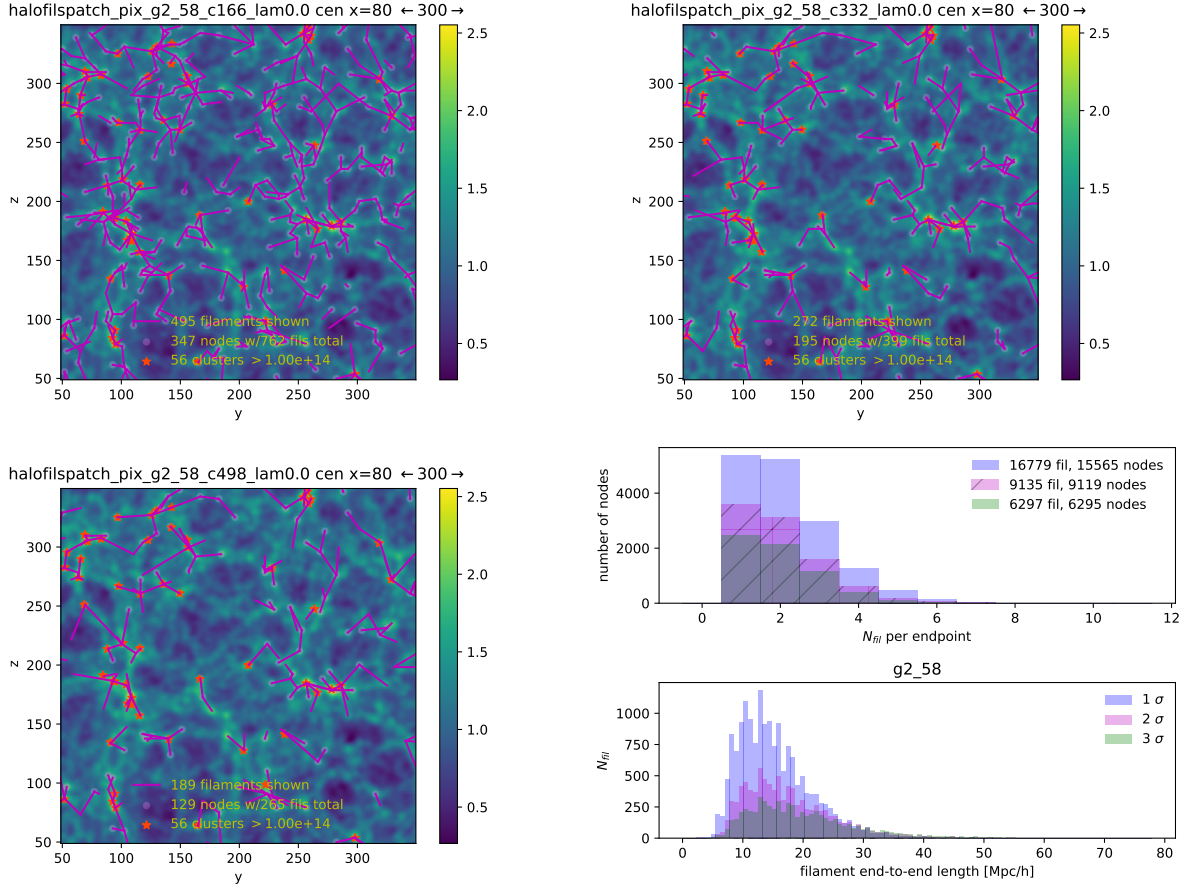


Figure 1. Webs with different DISPERSE persistence levels. Color denotes $\log(\text{density})$. The density slice is $30 \text{ Mpc}/h$ deep and $300 \text{ Mpc}/h$ wide, centered at position $(80, 200, 200) \text{ Mpc}/h$, and viewed down the x axis, with smoothing $2 \text{ Mpc}/h$. The 3 panels show DISPERSE nodes and filaments corresponding to persistence of 1σ (upper left), 2σ (upper right), 3σ (lower left). The grey-blue dots are DISPERSE node pixels, connected by filaments (magenta lines). At lower right are statistics for the full $500 \text{ Mpc}/h$ side box: the number of filaments per node, and distribution of filament lengths. With increasing persistence, the number of nodes, filaments, and connectivity go down, and the average filament length increases.

components, the Hessian based web finder uses eigenvalues $\lambda_1 \geq \lambda_2 \geq \lambda_3$ of the shear tensor $T_{ij} = \partial_i \partial_j \phi$, where ϕ is the gravitational potential (Zel’dovich 1970). The eigenvalues are calculated for each pixel from the smoothed density field. Every pixel is then assigned to a web component based on how many eigenvalues are $>$ or $<$ 0, nodes correspond to $(+++)$, filaments to $(++-)$, walls to $(+-)$ and voids to $(---)$. One can generalize to classifying eigenvalues being above or below (Forero-Romero et al 2009) some value λ_{th} , which then becomes an additional web parameter. To construct objects such as a node or filament from these individually labelled pixels, more assumptions are needed. In the following, every set of contiguous node pixels will be considered a separate Hessian “node” or “patch.” These patches will be used in one of the cluster-DISPERSE node matching methods below (which assigns Hessian patch regions to DISPERSE nodes lying within them). Even more assumptions would be required

to identify and construct Hessian based filament objects; this will not be pursued here.⁷

Again, both the DISPERSE and Hessian web classifications depend upon the smoothing length and pixel scale, parameters not intrinsic to the mass distribution itself, DISPERSE also depends upon persistence and the Hessian classification also depends upon λ_{th} .

A $30 \text{ Mpc}/h$ deep simulation slice is shown in Fig. 1, with DISPERSE nodes and filaments, for persistence 1σ , 2σ and 3σ (the smoothing is $2 \text{ Mpc}/h$). For these three DISPERSE webs, the distribution of DISPERSE node and filament counts, node connectivities, and filament lengths are intercompared in the box at lower right. The 3σ persistence DISPERSE web with smoothing $2 \text{ Mpc}/h$ will be used below when examples for a single parameter choice are shown. The $2 \text{ Mpc}/h$ smoothing is motivated by its frequent use (e.g., Hahn et al 2007a,b).

⁷ An example of a method to construct filament objects from a Hessian description is found in Pfeifer et al (2022).

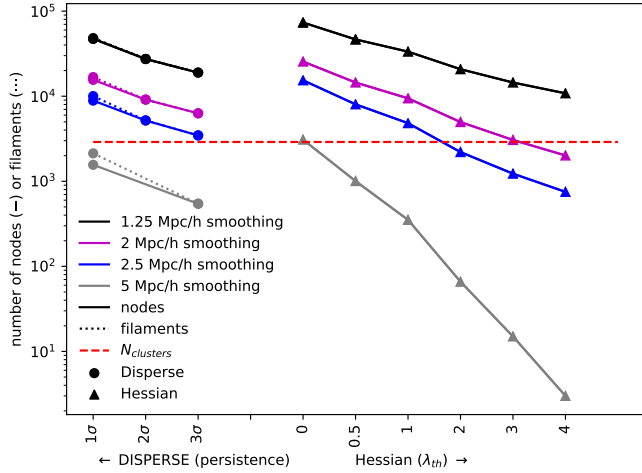


Figure 2. Node counts in different web descriptions, relative to the number of clusters, the 2898 massive halos with $M \geq 10^{14} M_{\odot}$ (red dashed line). For each smoothing (color), the left 3 points are the number of DISPERSE nodes (circles), ordered by increasing persistence. The right 5 points are the number of Hessian nodes (triangles), labeled by λ_{th} (in units of $\partial_i \partial_j \nabla^{-2} \rho / \bar{\rho}$). Dotted lines show the number of DISPERSE filaments, close to the number of nodes except for the 1 σ persistence, 5 Mpc/h smoothing.

2 ASSOCIATING CLUSTERS AND NODES

2.1 Nodes: counts and Hessian node patch properties

Before associating clusters and nodes, the first question is how many of each are present? Node counts are summarized for several Hessian and DISPERSE choices of parameters in Figure 2. The numbers of nodes are shown at left by circles for DISPERSE persistence of (1 σ , 2 σ , 3 σ) and at right by triangles for Hessian thresholds $\lambda_{th} = (0, 0.5, 1, 2, 3, 4)$. Color denotes the different (1.25, 2.0, 2.5, 5.0) Mpc/h smoothings. The red dashed line is the number of clusters.

For all the smoothings considered, not just the 2 Mpc/h example in Fig. 1, as DISPERSE persistence goes up, the number of nodes and filaments go down, and longer filaments become a higher fraction of all filaments (as the nodes become rarer and further apart). Often the number of filaments does not exceed the number of nodes by much, see Fig. 2.⁸

Similarly, the number of Hessian node patches decreases as the threshold λ_{th} eigenvalues must cross, in order to qualify as a node, increases. As mentioned earlier, DISPERSE nodes are single points in a single pixel, parameterized by position and density. The Hessian node patches have, in addition, a size, that is, the number of contiguous pixels classified as part of a given node. Larger Hessian patches are less frequent as the threshold λ_{th} increases and more frequent as smoothing increases.⁹

⁸ Within 0.4% except for 1 σ persistence, where N_{node}/N_{fil} drops from 98% to 73% as smoothing increases from 1.25 Mpc/h to 5 Mpc/h.

⁹ For $\lambda_{th} = 0$ and smoothing 1.25 Mpc/h, 40% of the Hessian nodes have only one pixel, while for the more restrictive $\lambda_{th} = 4$, 71% of the Hessian nodes only have one pixel. As smoothing

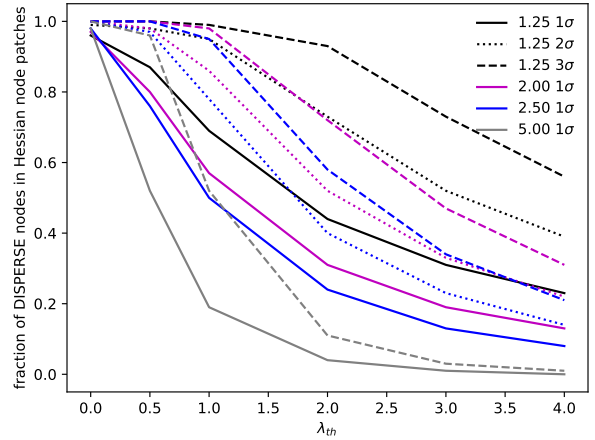


Figure 3. DISPERSE nodes and Hessian node patches: the fraction of DISPERSE nodes which have a corresponding Hessian node (via lying in a shared pixel), for DISPERSE persistence: 1 σ (solid), 2 σ (dotted), 3 σ (dashed). The color denotes Gaussian smoothing (1.25 Mpc/h, 2 Mpc/h, 2.5 Mpc/h, 5 Mpc/h) as indicated. For fixed λ_{th} , higher persistence and lower smoothing webs give a higher fraction of DISPERSE nodes matched to Hessian nodes.

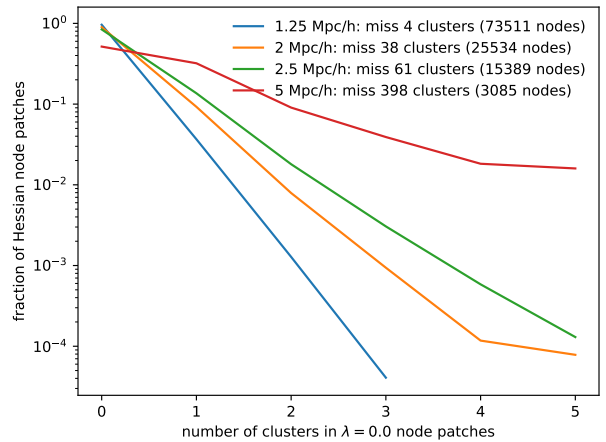


Figure 4. Clusters and Hessian node patches: the fraction (note the log scale) of $\lambda_{th} = 0$ Hessian node patches which contain a given number of clusters, as a function of Hessian web smoothing, or “node occupation distribution.” The Hessian patch nodes significantly outnumber the clusters except for the 5 Mpc/h smoothing. The numbers of clusters (out of 2898) not lying in any Hessian node patch, for each smoothing, are shown in the legend.

Looking ahead to matching clusters and DISPERSE nodes lying in the same Hessian node patch, in Fig. 3 the fraction of DISPERSE nodes which lie within (pixels which are part of) Hessian node patches is shown as a function of threshold λ_{th} and DISPERSE persistence. As the DISPERSE persistence

increases, fewer node patches have only one pixel, e.g., only 3% do so for smoothing 5 Mpc/h and $\lambda_{th} = 0$.

is raised, a higher fraction of DISPERSE nodes lie in Hessian node pixels for a given λ_{th} , that is, the definitions tend to overlap more often. Given the steep drop in the number of matched DISPERSE nodes to Hessian patches as λ_{th} is raised, in order to have more DISPERSE nodes available to match to clusters, only $\lambda_{th} = 0$ Hessian patches will be used hereon. As smoothing increases, a smaller fraction of DISPERSE peaks lie in Hessian patches for a given λ_{th} .

Turning to clusters, most Hessian nodes have no clusters lying inside them at all. However, because the Hessian patches can be large, in some cases with average radii from the maximum density point of 12-16 Mpc/h , a fraction of Hessian node patches contain several clusters. This allows one to construct a “node occupation distribution” (by clusters), shown for the four different Hessian web smoothings (again, $\lambda_{th} = 0$) in Fig. 4. That is, this is the fraction of Hessian node patches containing a given number of clusters (ranging from 0 to 5, except for 5 Mpc/h smoothing, with a maximum of 12). More clusters share Hessian patches (i.e., are in the same Hessian patch, together) and more clusters are missed, as the smoothing increases (legend, Fig. 4).

2.2 Associating clusters to nodes

A correlation between clusters and DISPERSE nodes is expected, but the relation is not necessarily expected to be one to one. In particular, the DISPERSE web finds critical points which are peaks (nodes, with a height difference requirement depending on persistence) and saddle points in ridges (filaments), and depends upon smoothing and pixel scales as well. Clusters have integrated density above some absolute scale (mass scale), and do not depend upon the smoothing and pixel scales.

Several ways to associate clusters to the DISPERSE nodes were considered and are compared below:

- “fixed” and “nearest”: if, for a given DISPERSE node, the cluster center is within some fixed distance of (“fixed”), or the cluster center is the nearest cluster center (“nearest”) within that fixed distance; the fixed distance is taken to be twice the smoothing
- “pix”: if the cluster center and the DISPERSE node lie in the same pixel
- “patch”: if the cluster center pixel is in the same Hessian node patch as the DISPERSE node pixel

Other matching methods using Hessian patches were considered, such as clusters being within a set distance from a Hessian node patch center or peak, or within a set distance from any pixel in a Hessian node patch, but all of these introduce more complexity, assumptions and difficulty in interpretation.

For matching clusters to DISPERSE nodes based upon distance (“fixed” and “nearest”), the choice of distance scale was guided by looking at the distance to the nearest DISPERSE node for each cluster (e.g., Fig. 5, upper right) and the distance to the nearest cluster for each DISPERSE node (Fig. 5, middle right), shown for the reference DISPERSE web with 2 Mpc/h smoothing and 3σ persistence. For all smoothings, there seems to be a clear subset of clusters with a DISPERSE node close by, roughly captured by using twice

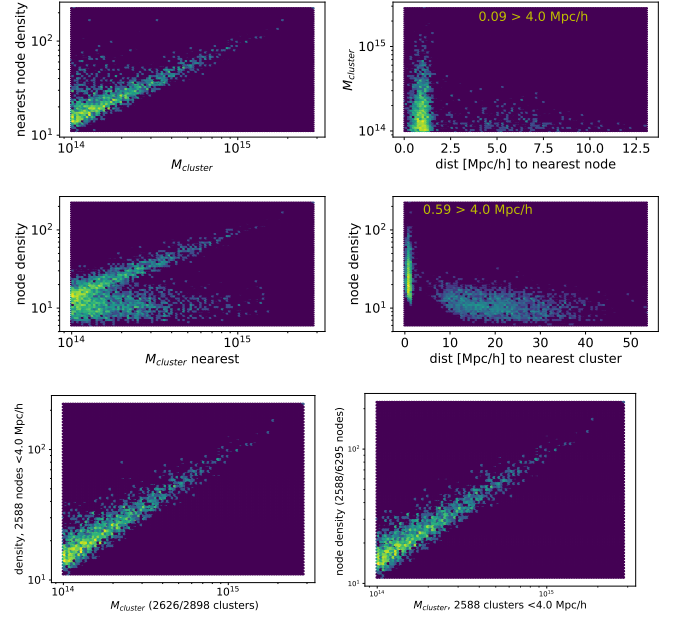


Figure 5. Relation between clusters and their nearest DISPERSE node, for 3σ persistence and smoothing 2 Mpc/h . At top, the nearest node for each of the 2898 clusters is shown. The low mass clusters are paired with nodes having a range of densities, and sometimes that association is weak, as the nearest node can be up to 15 Mpc/h away. Within twice the smoothing distance (4 Mpc/h), 9% of clusters do not have a DISPERSE node. At middle, the nearest cluster for each of the 6295 DISPERSE nodes is shown (there are many more nodes than clusters), which are sometimes $> 40 Mpc/h$ away. 59% of the 6295 DISPERSE nodes do not have a cluster within 4 Mpc/h . The lowest density nodes have a wide range of paired cluster masses. More than one cluster can have the same nearest DISPERSE node and vice versa. The color scheme for densities in each plot pixel is logarithmic. At bottom, by restricting to DISPERSE node-cluster pairs within twice the smoothing length, a cluster mass-DISPERSE node density relation is seen. At left, fixing the 2898 clusters and finding the closest DISPERSE node, at right, vice versa.

the smoothing scale as a distance cutoff.¹⁰ Restricting to only DISPERSE node-cluster pairs within twice the smoothing length, a DISPERSE node density-cluster mass relation is seen all the way down to the lowest DISPERSE node densities and cluster masses (Fig. 5, bottom).

More than one cluster can have the same nearest DISPERSE node and vice versa. The number of times the closest DISPERSE node to a cluster within the (twice smoothing) distance cut is already matched is < 25 for the 1.25 Mpc/h smoothing, dropping to 5 additional clusters for 2 Mpc/h smoothing with 1σ persistence and then becoming zero for larger smoothings or persistence. In contrast, the number of DISPERSE nodes whose nearest cluster is already matched rises with smoothing ($\sim 1, \sim 40, \sim 110, > 300$) for smoothings (1.25 Mpc/h , 2 Mpc/h , 2.5 Mpc/h , 5 Mpc/h). Both “fixed” and “patch”

¹⁰ The pixel scale of $\sim 2 Mpc/h$ seems relevant, as DISPERSE nodes are only defined on a grid with that resolution, i.e., DISPERSE node location changes on smaller scales do not reflect the underlying matter distribution on smaller scales. It was not clear how to take this into account.

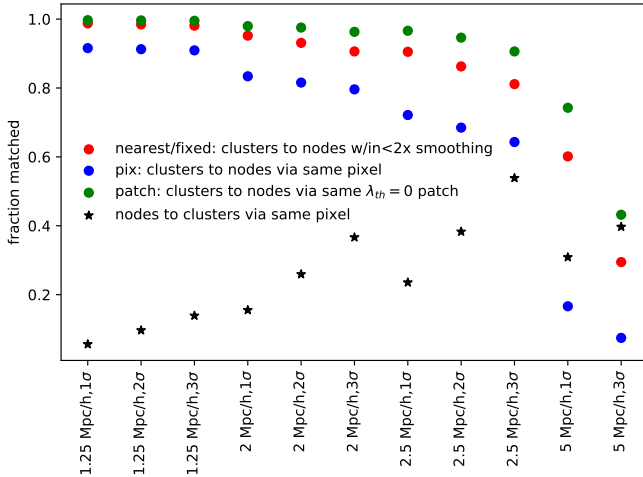


Figure 6. Fractions of clusters matched to DISPERSE nodes via the “nearest/fixed”, “pix”, “patch” methods, as a function of smoothings and persistence (1σ , 2σ , 3σ) and methods; clusters lying in the same $\lambda_{th} = 0$ Hessian patch (green dots, “patch”), lying within a distance of twice the smoothing length (red dots, “nearest” or “fixed”), and lying within the same pixel (blue dots, “pix”) as a DISPERSE node. The $\lambda_{th} = 0$ Hessian patch and the DISPERSE 1σ persistence $1.25 \text{ Mpc}/h$ smoothed nodes gives the most matched clusters (2889/2898). The “patch” method for higher λ_{th} values has fewer clusters matching DISPERSE nodes relative to all 3 methods shown. Stars refer to the fractions of DISPERSE nodes with clusters in the same pixel, matching via the “pix” method, a similar fraction (from 94% to 29%) of DISPERSE nodes do not have a cluster within $2 \text{ Mpc}/h$.

also do not necessarily associate a unique cluster to a given DISPERSE node (or a unique DISPERSE node to a given cluster, for patch), as they map all clusters in a given region to the same DISPERSE node.

The pixel matching method is unambiguous but can fail to match a cluster to a DISPERSE node if the cluster center is offset from the pixel containing the latter, even if the cluster itself extends into the DISPERSE node pixel. So although clearly defined, there are reasons to think it might be too restrictive.

Although for almost all DISPERSE webs there are many more DISPERSE nodes than clusters, not all clusters are matched to DISPERSE nodes. The fraction of clusters which are matched to DISPERSE nodes by each of the 4 methods above,¹¹ for the different DISPERSE webs, is shown in Fig. 6.¹²

¹¹ Note that “nearest/fixed” are two methods, in one case only one DISPERSE node is matched, in the other, all DISPERSE nodes within twice the smoothing are matched. For counting how many clusters have at least one match, these give the same result, and so are shown as the same point. However, the two cases correspond to different configurations more generally, so are counted separately, i.e. 36 webs are considered, in Fig. 7 below.

¹² One way of evaluating this matching is to compare how well finding DISPERSE nodes manages to find clusters, to how well different halo finders find the same object (cluster). In Fig. 17 of Knebe et al (2011), a halo finder comparison paper, the number of halos above $10^{14} M_{\odot}$ can differ by around 10% between some finders, comparable to or larger than the number of clusters missed by

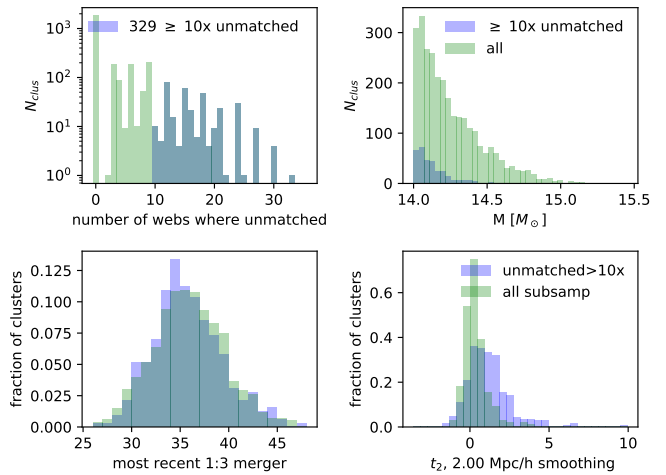


Figure 7. Properties of clusters, shown in blue, which are unmatched in 10 or more of the 36 combinations of DISPERSE webs and cluster matching methods (smoothing $< 5 \text{ Mpc}/h$). Upper left is the number times each cluster is unmatched for the 36 combinations (“nearest” and “fixed” are degenerate for this quantity). Upper right shows the full cluster mass distribution; the unmatched cluster mass distribution tends to be lower mass. The lower panels compare a mass matched sample of all clusters (lighter green) with the same 329 clusters unmatched for ≥ 10 of the 36 combinations (in blue). At lower left, the most recent 1:3 merger time step is perhaps slightly less recent for unmatched clusters (more recent is higher number). At lower right, $t_2 = \lambda_2 - \delta/3$ (calculated for smoothing $2 \text{ Mpc}/h$) seems higher for the unmatched clusters. Similar trends were seen for the (smaller number of) clusters which remained frequently unmatched when considering only matching via “nearest”, “fixed” and “patch” (i.e., dropping “pix”).

In contrast to the large number of matched clusters, most of the DISPERSE nodes are not matched to clusters (for example, stars in Fig. 6, for “pix” matching), although going to low enough halo or even subhalo mass would perhaps give at least one (sub)halo in the same pixel as every node. Increasing the fraction of matched DISPERSE nodes by raising persistence or smoothing causes the number of matched clusters to decrease.

Setting aside the two $5 \text{ Mpc}/h$ smoothed webs for the rest of this section, as their DISPERSE nodes miss significantly more clusters, there are 36 combinations of DISPERSE webs and matching methods. For these, a histogram of the number of times each cluster is unmatched (from 0 to 36 out of the 36 combinations) is shown in the upper left hand corner of Fig. 7. Over half of the clusters (1832/2898) were matched to DISPERSE nodes for every web and method. Dropping the “pix” method, which contributes 9 of the 36 variations, and is the most restrictive way to match clusters and DISPERSE NODES, 2248/2898 clusters, about 3/4, were always matched to DISPERSE nodes, by all remaining 3 methods.

One cluster was missed by every method, by dint of being slightly beyond the distance cutoff (of twice the smooth-

the “nearest/fixed” and “patch” methods in Fig. 6, except for the largest $5 \text{ Mpc}/h$ smoothing and the $2.5 \text{ Mpc}/h$ smoothing with 2σ or 3σ persistence. I thank C. Miller for suggesting this comparison and the reference to help make the comparison.

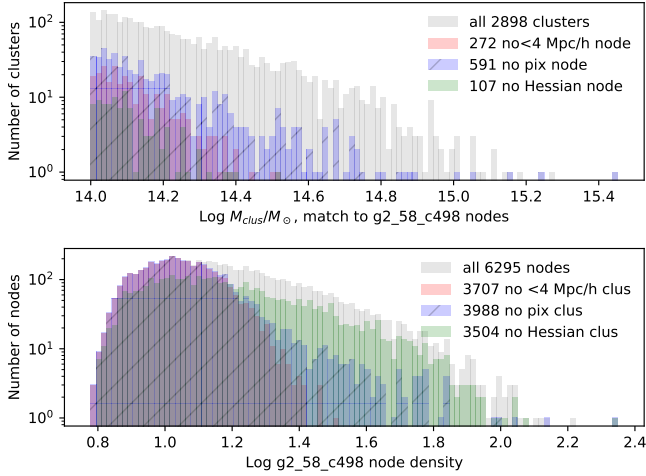


Figure 8. Cluster mass function (top) and DISPERSE node density function (bottom), grey, for the reference 3σ persistence $2Mpc/h$ smoothed DISPERSE web. In color are properties of clusters unmatched to DISPERSE nodes (top) and vice versa (bottom), via three matching methods. The three methods are lying within twice the smoothing length ($4Mpc/h$, “nearest”), lying in the same pixel (“pix”), or lying in the same Hessian node patch (“patch”). Unmatched clusters (top) missed by the “patch” and “nearest” methods seem to lie in the low mass range, while the many more clusters missed by the “pix” method ranged all the way to the highest mass. In comparison, almost all the low density DISPERSE nodes are missed by the “nearest” and “pix” method, but DISPERSE nodes missed by the “pix” method also go up to higher density. The “patch” method has fewer DISPERSE nodes unmatched to clusters, but many more of the “patch” unmatched DISPERSE nodes are at high density.

ing scale), while 79 (329) were not matched to DISPERSE nodes for 20 (10) or more web/method combinations (out of 36). Some characteristics of the 329 clusters which were unmatched for 10 or more of the 36 web/matching combinations are shown in Fig. 7. At upper right is their mass distribution (they tend to be lower mass). At lower left is the time of their most recent major (1:3) merger, which seems slightly earlier than for a random cluster subsample with the same mass distribution. For different underlying DISPERSE webs, the merger history difference is most pronounced for the smallest smoothing and increases as the maximum allowed distance for matching between clusters and DISPERSE nodes increases from twice the smoothing scale.

At lower right is the distribution, for the frequently unmatched clusters versus a random cluster subsample with the same mass distribution, of the middle component of “velocity shear” (Ludlow & Porciani 2011), $t_2 = \lambda_2 - \delta/3$. The t_2 distribution of the frequently unmatched clusters seems to be higher relative to the subsample of all clusters. (When considering clusters unmatched for a specific DISPERSE web matching, t_2 is calculated using the same smoothing scale as the DISPERSE nodes. For this figure, $2Mpc/h$ is used.) The “velocity shears” t_i , refer to whether local collapse is favored (if > 0) or impeded (if < 0) along a given axis, and these unmatched clusters seem to be in regions that have collapse favored along two axes more frequently ($t_2 > 0$) relative to all clusters. More frequent $t_2 > 0$ was also found for the initial

conditions of “peakless halos”, massive halos lacking a corresponding high mass peak in the initial conditions (Ludlow & Porciani 2011). The difference in t_2 between matched and unmatched clusters is largest for webs with smaller smoothing and for matching methods which produce fewer unmatched clusters. Samples of clusters which are further away from the nearest DISPERSE nodes tend to have the highest difference in t_2 from the matched clusters.

For DISPERSE nodes, those which are unmatched tend (slightly) to be lower density (an analogue of mass) for some smoothings and persistences, but it is harder to look at trends across different webs as the DISPERSE nodes themselves also vary between webs.

Looking at a single example, the reference DISPERSE web (3σ persistence and $2Mpc/h$ smoothing), Fig. 8 shows the mass distributions for unmatched clusters (top) and density distributions for unmatched DISPERSE nodes (bottom), as the cluster-DISPERSE node matching methods are varied. The mass distribution of unmatched clusters seems similar for the three matching methods, with the method missing the most clusters extending to the highest mass clusters. In contrast, the density of unmatched DISPERSE nodes seems significantly different for the “patch” method compared to the other two, in particular, the “patch” (i.e., Hessian) method does match some of the low density DISPERSE nodes to clusters, while the other two methods seem to result in almost all of the low density DISPERSE nodes being missed.

In summary, DISPERSE nodes can be matched to clusters in several ways. For the 9 DISPERSE webs, the 4 matching methods, and smoothing $< 5Mpc/h$, over half of the clusters always have a matched DISPERSE node. Over 3/4 of the clusters have a DISPERSE node match if the “pix” matching method, exact pixel overlap of DISPERSE nodes and cluster centers, is not considered. The clusters without DISPERSE nodes in at least 10 of the 36 matching methods and underlying DISPERSE webs, $\sim 11\%$, tend to be lower in mass, have perhaps a earlier most recent major merger, and more likely a higher t_2 than the full cluster sample. (Similar results were found for the 1/4 clusters which didn’t always have a DISPERSE node match for the combination of only the “fixed”, “nearest”, and “patch” methods.) Clusters and their nearest DISPERSE nodes within twice the smoothing length of each other have a DISPERSE node density-cluster mass relation.

3 CLUSTER-CLUSTER FILAMENTS

3.1 Assigning filaments

The four methods above associate DISPERSE nodes with clusters for any DISPERSE web. As DISPERSE nodes are linked by DISPERSE filaments, clusters matched to DISPERSE nodes can be linked to each other if their matched DISPERSE nodes share a filament. Each underlying DISPERSE web and combined cluster-DISPERSE node matching method produces a different set of filament assignments to cluster pairs. The cluster distribution remains fixed: these filaments are the parts of each underlying DISPERSE web “picked out” by clusters.

In practice, filaments are assigned to cluster pairs by first restricting the DISPERSE web to DISPERSE nodes which have matches to clusters. DISPERSE nodes which are unmatched to clusters have their filaments either reassigned (eventually to

cluster matched DISPERSE nodes) or dropped. This restriction begins by sorting unmatched DISPERSE nodes according to the number of filaments which end on them. Unmatched DISPERSE nodes with just one filament are simply dropped, and then a check is done again to find whether any new unmatched DISPERSE nodes with only one filament were created, if so, these are dropped as well and this process is repeated until no more unmatched DISPERSE nodes with just one filament remain. To drop unmatched DISPERSE nodes with more than one filament coming out, any pair of filaments meeting at the same unmatched DISPERSE node with an angle of more than 120 degrees is replaced by a single filament bypassing the unmatched node. After this new filament assignment, the unmatched DISPERSE node is dropped. If the angle is smaller, the two filaments ending on the DISPERSE node are just dropped. This is to catch the cases where two cluster matched DISPERSE nodes are linked via an intermediate unmatched DISPERSE node, where the bending is not too large at the dropped DISPERSE node. (However, at times several of these dropped DISPERSE nodes can be strung together, leading to a single very bent filament.) Unmatched DISPERSE nodes are dropped starting with those which have only two filaments (repeated until all instances are gone) and then going to higher multiplicities. For the higher multiplicities, as dropping unmatched DISPERSE nodes can change the number of filaments coming out of the remaining DISPERSE nodes, unmatched DISPERSE nodes which have lost filaments since the ordering according to filament number are passed over until all multiplicities are considered. At this point, all remaining unmatched DISPERSE nodes are ordered again by filament number, and the process repeats until all unmatched DISPERSE nodes are gone.

This produces a map of cluster matched DISPERSE nodes and their filaments. A second map was also made, where only filaments directly connecting matched DISPERSE nodes were kept, dropping the filaments interpolating through unmatched DISPERSE nodes. Unless specified otherwise below, the cluster-cluster filaments below also include those found via interpolation. Dropping the interpolated filaments reduces the number of filaments between 8% and 50%, depending on web and matching variation, with the smallest smoothing and persistence having the most interpolated filaments.

The next step is to replace DISPERSE nodes which are connected by filaments with their matched clusters. Because the cluster to DISPERSE node matching is not always one to one, this step can be ambiguous. A matched node might have two clusters associated with it, or two matched nodes might have the same nearest cluster. (The number of occurrences of multiple clusters within a single Hessian node patch, used in the “patch” method was shown in Fig. 4.) And again, matching the nearest cluster and DISPERSE node within a smoothing dependent distance cut can also lead to degeneracies because the nearest DISPERSE node to a cluster might not be the nearest cluster to that DISPERSE node. Two options are used, and appear to give similar results. In one case, “nearest,” if two clusters both have the same nearest node, within the distance cutoff, they are linked to each other with filaments, and if two nodes claim the same cluster as their nearest cluster, and another cluster claims either node, the two clusters are also linked via filaments. A second way to proceed, “fixed dist,” is to match every cluster within the smoothing dependent

distance cut to the node, and if there is more than one, to connect these clusters to each other with filaments.

At the end of this construction, every cluster has a list of other clusters to which it is connected via filaments. There is a different set of cluster-cluster filament pairs for each combination of cluster-DISPERSE node matching method and underlying original DISPERSE web.

3.2 Comparing different cluster-cluster filament assignments

An underlying DISPERSE web is shown, along with two cluster pair filament assignments based upon it, in Fig. 9. As in Fig. 1 this is for a 30 Mpc/h density slice, with the original DISPERSE web from Fig. 1 at upper left (magenta filaments, smoothing 2 Mpc/h with 3σ persistence), the filaments produced from the “nearest” method at upper right and the filaments produced by the “patch” method at lower left (cluster DISPERSE node matching methods are described in §2.2). The matched clusters are red stars, unmatched clusters are yellow stars, and the cluster-cluster filaments are shown as black lines. At lower right are the statistics of all the filament assignments based upon this particular DISPERSE smoothing and persistence.

Included in the comparison of cluster-cluster filament pairs in Fig. 9 (lower right panel) is a cluster based minimal spanning tree web (some variants are in, e.g., Barrow et al (1985); Park & Lee (2009); Alpaslan et al (2014); Pereyra et al (2020)). This is included for comparison because it is a web constructed directly from the clusters themselves, by choosing each cluster as a web node. It is created by ranking cluster pairs according to some property (two ranking properties which have been used for halo/galaxy based webs are the distance between them, Alpaslan et al (2014), used here, or $M_1 M_2 / r^2$ Pereyra et al (2020)). Filaments are then assigned to cluster pairs in ranked order, omitting any pair where both proposed endpoints are already connected to filaments, to get $N_{clus} - 1$ filaments.

In the filament assignments for the example shown in Fig. 9, with an underlying 2 Mpc/h smoothing, 3σ persistence DISPERSE web, some general trends can be seen. As the cluster-cluster filament pairs only have 2898 clusters to serve as possible endpoints, versus the 6295 original DISPERSE web nodes, there are fewer cluster-cluster filaments (filament counts are listed in the legend of Fig. 9, top half of lower right panel). There are also some longer cluster-cluster filaments relative to those of the underlying DISPERSE web, likely due to the merging of shorter filaments when interpolating between cluster matched DISPERSE nodes. The filaments tend to be shorter in the cluster based minimal spanning tree web, as the shortest distance pairs were chosen to have filaments.

More generally, in the original DISPERSE webs, and the minimal spanning tree webs, every cluster has at least one filament (although the minimal spanning tree web tends to be more tree than “web” like, as it does not have closed loops). The cluster-cluster filaments do not result in a fully connected object, in particular, there are clusters with no filaments, either because they have no associated DISPERSE nodes (see Fig. 6) or because their matched DISPERSE node didn’t have filaments to another matched DISPERSE node. (However, some unmatched clusters acquire filaments in the “fixed” method for assigning filaments, even though they

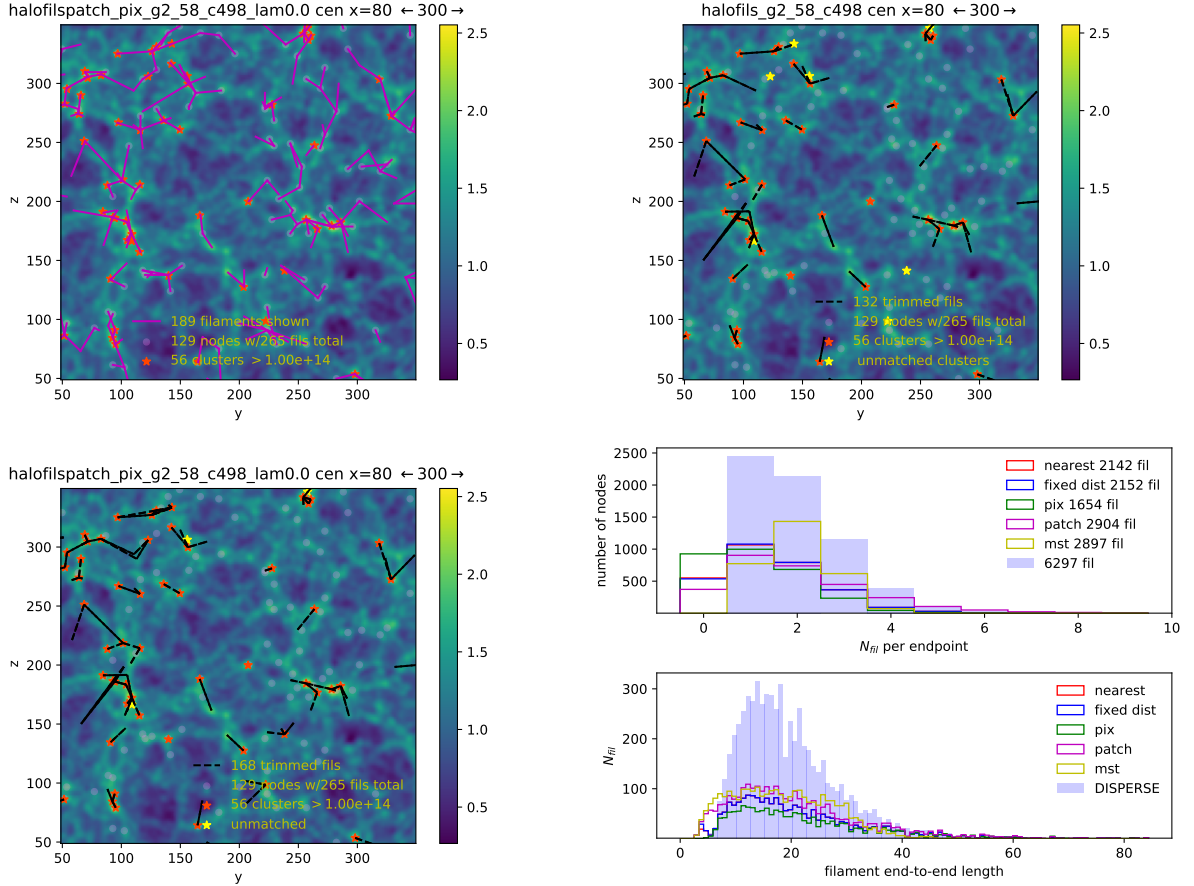


Figure 9. Comparisons of a $30 Mpc/h$ slice for filaments resulting from the 3σ persistence, $2 Mpc/h$ smoothed DISPERSE web, overlaying a (logarithmic) density map (from Fig. 1). Interpolation through unmatched DISPERSE nodes is done as described in the text. At upper left is the original DISPERSE web. The (magenta) DISPERSE filament endpoints are DISPERSE node pixels. The red stars are clusters. For the cluster-cluster filaments, unmatched clusters are yellow stars, and the black lines show cluster pairs which are connected by using their matched DISPERSE nodes and either the “nearest” method (upper right) or “patch” method (lower left), described in §2.2. Log scale is used for density. At lower right are statistics for all the different matching methods described in §2.2 plus the cluster based minimal spanning tree (“mst”) described in the text. The top plot in this panel is the number of filaments per cluster (with total filaments per method in the legend), the bottom plot is the filament length distribution. All maps have the same clusters and original fixed underlying DISPERSE web (its statistics are shown as shaded bars, repeated from Fig. 1). Clusters can have no filaments due to being unmatched to a DISPERSE node or by having their matched DISPERSE node not connected by filaments to other cluster-matched DISPERSE nodes (either directly or via dropped DISPERSE nodes).

don’t directly have associated DISPERSE nodes.) Considering all the cluster-cluster filament pairs, based upon all the different DISPERSE webs, the fraction of clusters with no filaments (for either of these reasons) is highest for pixel matching (“pix”), and lowest for Hessian node patches (“patch”). For “patch”, “nearest”, “fixed dist,” for smoothing below $5 Mpc/h$, the fraction of clusters with no filaments lies between $\sim 10\%$ $\sim 25\%$, while for “pix” the number of unlinked clusters was above 30% for all smoothings. The $5 Mpc/h$ smoothing reached 95% unlinked clusters (for “pix”) and more generally was worse for linking clusters for all methods. In the 36 cluster-web matching combinations with smoothing $< 5 Mpc/h$, 47 of the 2898 clusters are never connected via a filament to another cluster. If filaments aren’t interpolated across unmatched DISPERSE nodes, this goes up to 152 clusters.

4 CLUSTER PAIRS

4.1 Cluster pairs with and without filaments

All of these sets of inherited cluster-cluster filaments, from each of the 36 DISPERSE web-matching combinations, start with the same set of clusters. One way of thinking about the cluster-cluster filaments which appear, based upon a particular matching method and underlying DISPERSE web, is as an operation on the distribution of cluster pairs which selects those pairs which are linked. (Given the huge numbers of clusters with no filaments when $5 Mpc/h$ smoothing is used, these DISPERSE webs and their associated cluster-cluster filament pairs will not be discussed in this section.)

Of the over 420,000 cluster pairs in the box, only 5841 pairs have a filament in any of the 36 web variations. If interpolation is dropped, that is, only underlying DISPERSE web filaments with both ends lying on cluster matched DISPERSE

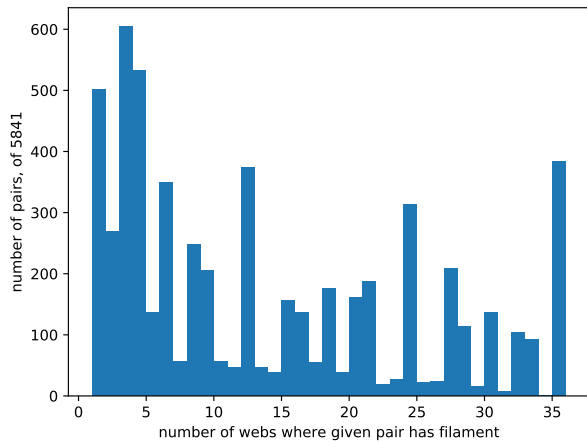


Figure 10. Frequency of cluster pairs with filaments. The number of times a given cluster pair has a filament, out of the 36 persistence/smoothing/matching combinations; 383 pairs had filaments in all 36. Only the 5841 cluster pairs linked with a filament in at least one of the 36 cluster- web matching combinations are shown.

nodes are kept, only 4440 cluster pairs ever have filaments. The distribution of how often each pair appears in these 36 web variations is shown in Fig. 10. Of these, 383 cluster pairs have filaments in every web, and these tend to be at smaller separation, e.g., between $10\text{--}20\text{ Mpc}/h$, although one cluster pair which always has a filament is separated by over $65\text{ Mpc}/h$. Slightly fewer than $1/5$ of the total number of pairs which were ever linked have filaments in most (i.e., at least $3/4$ of the 36 web persistence/smoothing/matching combinations; a bit more than half of the $1/5$ frequently linked cluster pairs correspond to filaments directly, not interpolated, between two cluster matched DISPERSE nodes). About $1/3$ of the cluster pairs ever having filaments only have them rarely (for ≤ 4 of the 36 combinations), while almost half have filaments only for ≤ 9 of the 36 persistence/smoothing/matching combinations. Thus, the 36 ways of assigning filaments to cluster pairs produce 36 sets of mostly non-coinciding cluster pairs with filaments. The rarest pairs seem to occur for “patch” matching, and for the largest smoothing, likely because “patch” can match many clusters across a large region with the same DISPERSE node or nodes.

Some trends appear in the pairs of clusters which are linked by filaments. As might be expected, clusters which are closer together are more likely to have a filament between them. In more detail, for these 36 webs, the fractions of cluster pairs which are connected by a filament, as a function of separation, are shown in Fig. 11. A dip in probability for somewhat close pairs is noticeable for the “nearest” and “fixed dist” filament assignments to cluster pairs, for smoothings $2, 2.5\text{ Mpc}/h$, although it is slightly present in the “patch” web as well.¹³

¹³ As clusters matched to the same DISPERSE node are linked by filaments, increasing the radius within which clusters and DISPERSE nodes are matched would remove the drop in number of linked cluster pairs, however, this dip is at the scale where nearby clusters tend to appear, so changing the matching radius would also tend to match more cluster pairs to a single DISPERSE node. Another

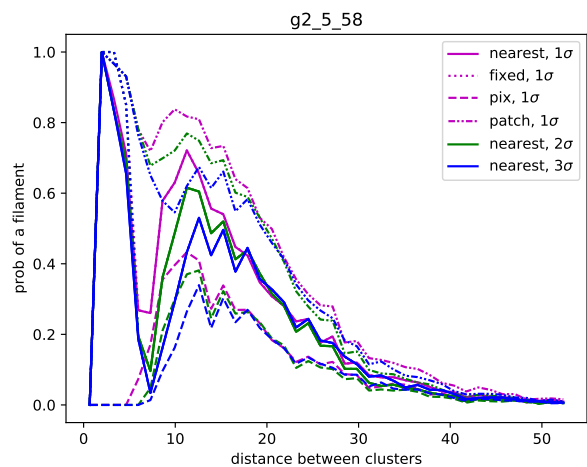
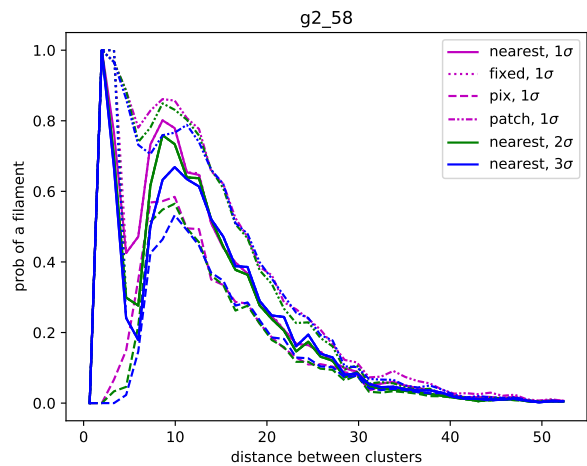
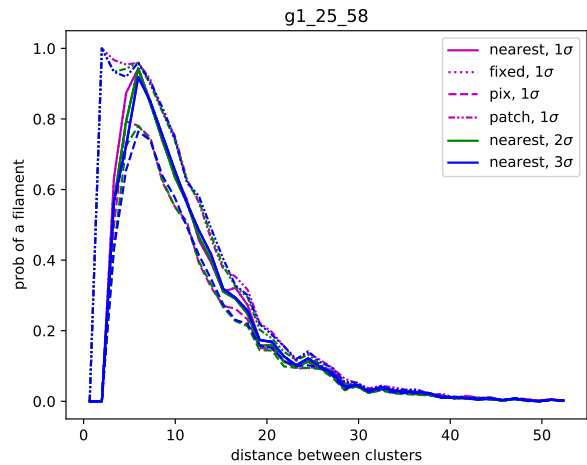


Figure 11. Fraction of cluster pairs with a filament as a function of cluster separation. The panels, top to bottom, correspond to smoothing lengths ($1.25\text{ Mpc}/h, 2\text{ Mpc}/h, 2.5\text{ Mpc}/h$). Line types distinguish cluster-DISPERSE node correspondence, color denotes DISPERSE persistence chosen. The Hessian patch matching between clusters and the DISPERSE web gives the simplest relation between filament likelihood and cluster separation, roughly less likely as separation increases, although for all webs based on smoothing above $1.25\text{ Mpc}/h$ there are additional features as a function of cluster separation.

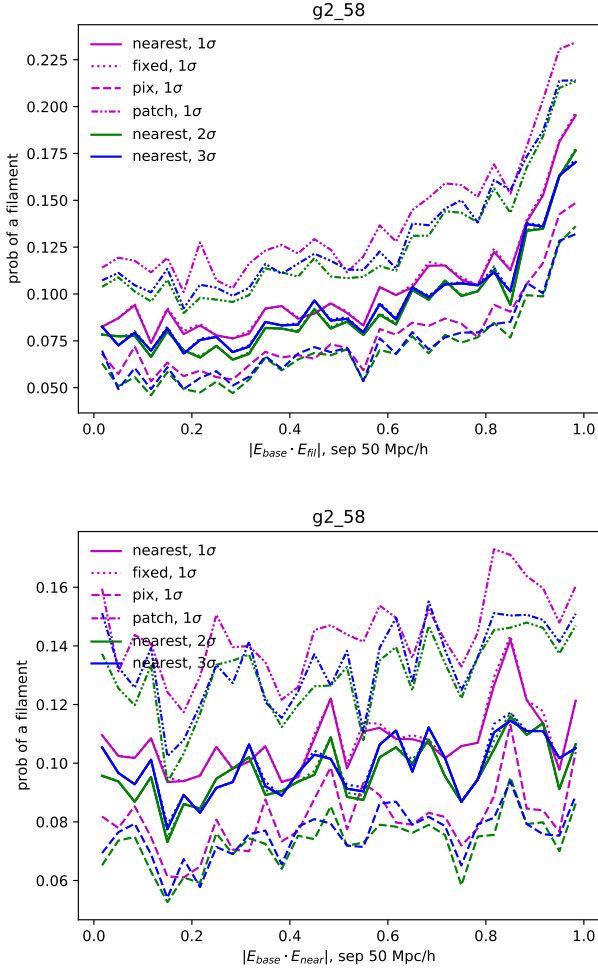


Figure 12. Fraction of cluster pairs separated by less than ~ 50 Mpc/h which have a filament, for different cluster to node matching methods as described in §2.2. Top: as a function of alignment of a cluster axis and cluster-cluster pair axis. Bottom: as a function of alignment of the two cluster pair endpoints. Smoothing length for both is $2 Mpc/h$. Again, line types distinguish cluster-DISPERSE node correspondences, color denotes chosen DISPERSE persistence.

For a given separation bin, cluster pairs with filaments were a minority of cluster pairs beyond $15\text{--}20 Mpc/h$ separations for any given separation.

Pair separation is the strongest indicator of whether a cluster pair is likely to be linked (but not sufficient information, as seen in Fig. 11). Alignments of the clusters’ long axes are another property that is expected to make a filament more likely (Bond, Kofman & Pogosyan 1996; Bond & Myers 1996). Taking pairs with separation less than $\sim 50 Mpc/h$, the fraction of linked pairs did not seem to have a strong dependence upon cluster-cluster axes alignment (e.g., bottom of Fig. 12, which for $2 Mpc/h$ smoothing shows only perhaps a slight increase, and seems slightly stronger for smaller smoothing).

possibility is to add yet another parameter in creating the filament assignments for “nearest” and “fixed”, a separate minimum radius within which all clusters are linked.

However, when the cluster-cluster pair axis was aligned with either cluster axis, a filament was present around twice as often as when these two axes were perpendicular to each other (although still only $\leq 25\%$ of the time, largest for the largest smoothing), some examples are shown in Fig. 12, at top.

Instead of looking at pair features one-by-one to see if a filament is present, machine learning can try to answer the classification problem (given a pair, is there a filament present or not) using a combination of features. Some methods also assign “importance” of each feature to the classification. Using the Random Forest classifier, “out of the box”¹⁴, the relative importance of the features of distance, cluster-pair axis alignment, cluster-cluster alignment, and rank, i.e. how many clusters were closer to the endpoint cluster than the other endpoint of the pair, were considered for all pairs below a fixed separation $\sim 50 Mpc/h$. Pair separation was, as expected, the most “important” feature, followed by rank (highly correlated with pair separation). When considered along with pair separation, cluster-cluster alignment and cluster-pair axis alignment were both approximately of the same “importance,” in contrast to the differing dependence seen when these were considered on their own in Fig. 12. It is possible that considering cluster alignment separately from cluster separation, as in Fig. 12, weakened the signal. It is also true, however, that for many cases, the machine learning success of matching filaments to pairs was not that good (above 8% mismatch for 11/36 of the filament assignments to cluster pairs), so it might be that more tuning is needed to use this approach, or that the presence of a filament is not amenable to being predicted by these (few) parameters. The AdaBoost classifier was also tried¹⁵, but did quite poorly on some of the 36 variations of cluster-cluster filament pair assignments.

Conversely, DISPERSE filaments with higher density at their critical points are also more likely to have matched cluster pairs, perhaps in part because they are the “low” points relative to higher density nodes. The analogous plots to Fig. 11 for filaments (what fraction of filaments of a given length are associated with a cluster pair) show that short distance filaments ($< 5\text{--}10 Mpc/h$) are more likely to have pairs. However the fraction of filament pairs matched to cluster pairs then only decreases slowly out to $40\text{--}50 Mpc/h$, unlike the sharp decrease in the fraction of matched cluster pairs with increased separation in Fig. 11.

4.2 Subhalo counts and halo mass density perpendicular to cluster pairs

One can look at profiles of different quantities perpendicular to the axis between cluster pairs, both those with and without filaments, for any web definition. If the cluster pair is connected by a filament, this is the filamentary radial profile of that quantity. Profiles for two quantities are shown for all cluster pairs up to some maximum separation, in Fig. 13 for the (11996, 20906, and 33842) cluster pairs with separations less than ($40 Mpc/h$, $50 Mpc/h$, $60 Mpc/h$), respectively. At left is the profile in subhalo number counts (in principle

¹⁴ RandomForestClassifier(max_depth=5, n_estimators=10, max_features=1), imported from sklearn.ensemble, described in <https://scikit-learn.org/stable/modules/ensemble.html>

¹⁵ AdaBoostClassifier(), also from sklearn.ensemble

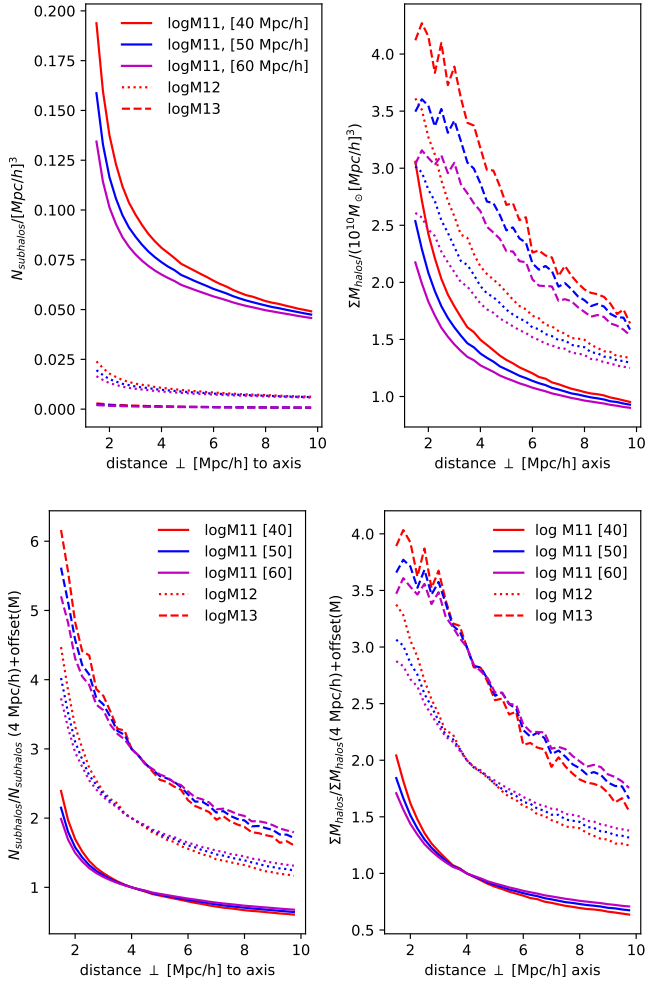


Figure 13. Enhanced density of subhalo counts (left) or halo mass (right), between cluster pairs, for (sub)halo masses $10^{11} - 10^{12} M_{\odot}$ (solid), $10^{12} - 10^{13} M_{\odot}$ (dotted) and $10^{13} - 10^{14} M_{\odot}$ (dashed). Top: the radial subhalo number density (left) and mass density (right) perpendicular to the line linking all pairs of neighboring clusters separated by $\leq 40 Mpc/h$ (red), $50 Mpc/h$ (blue), and $60 Mpc/h$ (magenta), with 11996, 20906, and 33842 cluster pairs respectively. The halo masses are placed at the halo center (treated as point masses). Below, counts and mass density rescaled by value at $4 Mpc/h$, and then multiplied by $\log_{10} M_{min}/10^{10} M_{\odot}$, to set apart the different mass populations. The minimum distance from the cluster-cluster axis is taken to be $1.5 Mpc/h$ to avoid numerical issues.

these would be associated with galaxies in a semi-analytic model), at right are the halo mass densities (where the mass of each halo is located at the halo center, i.e., the halo profile is neglected). Different subhalo infall mass (at left) and halo mass ranges (at right) are separated out, ($10^{11} M_{\odot} - 10^{12} M_{\odot}$, $10^{12} M_{\odot} - 10^{13} M_{\odot}$, $10^{13} M_{\odot} - 10^{14} M_{\odot}$), as indicated. The two panels below show the profiles rescaled to their values at $4 Mpc/h$ and then shifted to separate out the different subhalo (at left) and halo (at right) mass ranges. Pairs separated by more than $60 Mpc/h$ are omitted, ranging from 0.3% to 6% of the cluster pairs with web-assigned filaments. As can be inferred from Fig. 11, these omitted filament pairs are a very

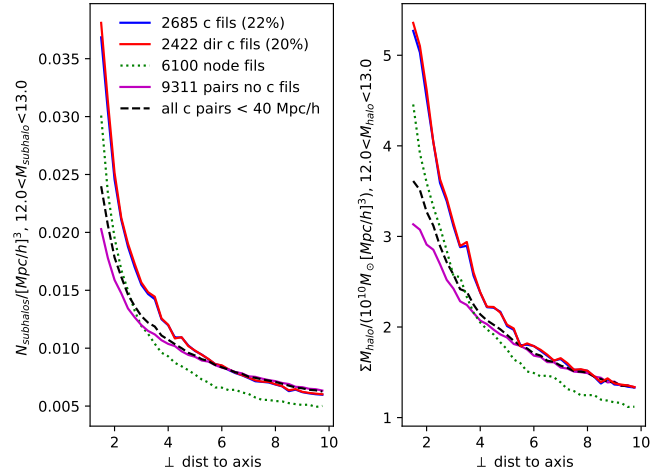


Figure 14. Example of the radial subhalo number count density (left) and halo mass density (right), for subhalo mass or halo mass respectively in the range $10^{12} M_{\odot} - 10^{13} M_{\odot}$, perpendicular to the line connecting cluster or DISPERSE node pairs with separation $\leq 40 Mpc/h$. The different pairs are clusters connected by filaments either directly (“dir c”, red solid line) or also via interpolation (“c”, blue solid line), not connected by filaments (bottom magenta line), all cluster pairs (black dashed, same curve as in Fig. 13) and DISPERSE nodes connected by filaments (dotted line). The underlying DISPERSE web was for $2 Mpc/h$ smoothing and 3σ persistence, with matching to clusters via the “patch” method. The filament profiles are closer to $1/r$ than the $1/r^2$ seen for other definitions by Colberg, Krughoff & Connolly (2005); Aragon-Calvo, van de Weygaert & Jones (2010).

small fraction of all large separation pairs. (Larger fractions of long filaments appeared with larger web smoothings.) The mass density is highest for the highest mass halos, and smallest for the pairs with the largest separation (presumably in part because larger pair separations result in including more pairs with no filaments).

For cluster pairs with filaments, several profiles corresponding to an underlying DISPERSE web with $2 Mpc/h$ smoothing, 3σ persistence, matched to clusters via “patch,” are shown in Fig. 14. The red and blue lines indicate the profiles for cluster pairs assigned filaments which interpolate through an unmatched DISPERSE node which are either kept (“c” files) or dropped (“dir c” files), the two profiles are not that different. Also shown is the average profile between all cluster pairs with the same maximum separation and subhalo minimum mass, and the average profile for the cluster pairs without a filament (slightly lower than the average profile). The DISPERSE node pair profile, dotted line, is between all DISPERSE node pairs in the corresponding web. For $r > 2 Mpc/h$ and visually detected filaments, Colberg, Krughoff & Connolly (2005) found a $1/r^2$ profile, similar fall off was found by Aragon-Calvo, van de Weygaert & Jones (2010) for a multiscale web finder. The average counts and mass profiles averaged over cluster filament pairs tended to be closer to a $1/r$ profile, with the stacked halo mass profile seeming slightly shallower than the counts profile. This might indicate some issue with the assigned filaments, either in how they are chosen, or the fact that filaments are taken to be straight between cluster pairs, which might be washing out some of the radial

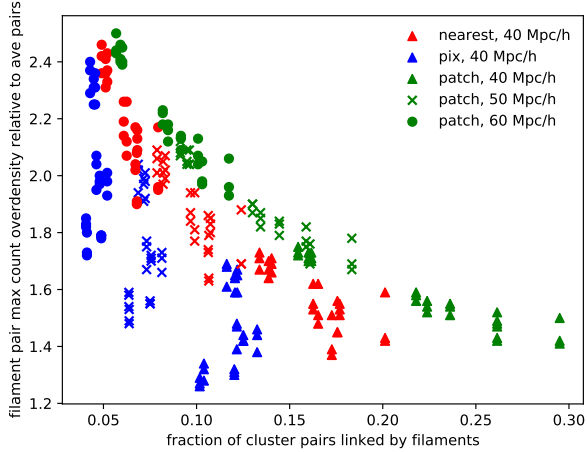


Figure 15. For the 36 combinations of DISPERSE web and cluster matching, the ratio of the maximum of the average filament pair profile peaks (for counts) over the average pair profile peak, as a function of the fraction of all cluster pairs which are filaments for that given combination. The general trend within a matching method is that larger fraction of pairs with filaments have less enhancement of the peak density over that of the average, as is expected. Lengths are denoted by shape, triangles are for maximum length 40 Mpc/h , crosses for 50 Mpc/h and circles for 60 Mpc/h . Shorter maximum lengths have higher fractions of cluster pairs linked by filaments. Points further towards the top are for smaller smoothing and higher mass subhalos.

structure. In the Colberg, Krughoff & Connolly (2005) filament catalogue, only 38% of the filaments were straight lines between the cluster endpoints. For the cluster pairs which mapped directly to DISPERSE filaments, with no interpolation, the offset between the line connecting the cluster (or DISPERSE node) endpoints and the filament centers (the saddle critical points provided by DISPERSE) had a median value ranging from 1-3 Mpc/h for the different web and matching variations.

As the count profiles tend to have a similar shape, one can characterize the filament enhancement of counts relative to counts around all cluster pairs with the same separation and subhalo mass ranges at a given distance from the cluster pair axis, chosen here to be 1.5 Mpc/h . The distribution of this filament associated density enhancement is shown as a function of the fraction of cluster pairs linked by filaments in Fig. 15. (As most of the cluster pairs don’t have filaments, the difference between profiles for the unlinked cluster pairs and all cluster pairs for maximum lengths $\geq 40Mpc/h$ is much smaller than that between linked and all cluster pairs.) The fraction of cluster pairs which have filaments goes down with increasing maximum cluster separation, and decreases as well as with more restrictive ways of matching clusters to filaments, ranging from $\sim 30\%$ of the pairs for one instance of “patch” and 40 Mpc/h separation, to 2% of the pairs for “pix” and 60 Mpc/h separation, roughly integrals of the distributions shown in Fig. 11. There tends to be less density enhancement relative to all pairs as the fraction of pairs which are filaments increases, as is expected, and the enhancement also tends to be lower for the “pix” matching and highest for the “patch” matching, as can be seen in Fig. 15. The en-

hancement relative to all pairs is larger for the higher mass tracers, expected from higher mass having higher bias.

On average, cluster pairs with DISPERSE web assigned filaments were a relatively small fraction of close cluster pairs. Nonetheless, the average subhalo count density found here, around 1.5 Mpc/h from the cluster-cluster line and irrespective of whether a filament was present, was enhanced by a factor of around 3 relative to its value $\sim 10 Mpc/h$ away from the line. Pairs with filaments assigned for any of the 36 combinations had maximum subhalo counts ranging from ~ 5 -8 times the subhalo counts $\sim 10 Mpc/h$ away from the center.

Subhalo count profiles and halo mass profiles were also calculated for DISPERSE node pairs connected by filaments, one of which is shown in Fig. 14 for the corresponding underlying DISPERSE web. There are several uncertainties and subtleties in calculating DISPERSE filament profiles. The DISPERSE node filaments are taken to run straight between the two nodes, discarding the shape information provided by DISPERSE. In addition, the DISPERSE nodes are defined for pixel (2 Mpc/h side) averaged densities, so that actual density peaks, if present, might be anywhere in the pixel, and are likely offset with respect to the few discrete positions the DISPERSE nodes take. In practice, the DISPERSE filament node pair profiles are stacked just as those for cluster pairs. The subhalo count peak (at 1.5 Mpc/h) overdensity between DISPERSE nodes ranges between 0.6 and ~ 2 of its counterpart for all cluster pairs (going up to the same maximum separation), with the highest relative values corresponding to the largest maximum separation pairs and longest DISPERSE filaments. For halo mass overdensity, the ratio ranged from 0.6 to 2.6 for the peak (again at 1.5 Mpc/h) for DISPERSE node pairs connected by filaments relative to all cluster pairs, again with the samples including the longest filaments and largest cluster separations giving the largest values. This increase was likely in part due to large separation cluster pairs being less likely to have filaments between them.

5 SUMMARY AND DISCUSSION

Here, the largest mass halos in the universe, clusters $10^{14}M_{\odot}$ and above, were matched to nodes in cosmic webs created using the web finder DISPERSE on pixel overdensities in a fixed time N-body simulation box. Filaments between cluster matched DISPERSE nodes were assigned to their corresponding cluster pairs.

DISPERSE was chosen because of its public availability and its frequent use, and applied to 4 smoothings of the underlying dark matter, the largest of which (5 Mpc/h) matched too poorly to clusters to be usefully studied in much detail. For the remaining smoothings, 3 values of the DISPERSE persistence parameter were considered, resulting in 9 different DISPERSE webs based upon the same underlying smoothed simulation.

In each of these 9 webs, clusters were matched to nodes by assigning a volume to the DISPERSE nodes via 4 methods, and then seeing if the cluster lay within this volume. Volumes were given by the pixel of the DISPERSE node ($\sim 2 Mpc/h$), or a twice smoothing radius sphere around the DISPERSE node, or within the same Hessian node “patch” (contiguous pixels all classified as nodes via the Hessian method). No method matched every cluster to a DISPERSE node, but about half of

the clusters had a matched DISPERSE node for every method, in all 9 underlying DISPERSE webs, and 3/4 had matches if the most restrictive matching (lying in the same pixel) was dropped. The clusters matched to DISPERSE nodes for the most methods and underlying DISPERSE webs tended to have higher mass and lower “velocity shear”, and, perhaps a higher likelihood of recent 1:3 mergers. High density DISPERSE nodes were more likely to have a matched cluster.

For every DISPERSE web, there generally appeared to be a distinct population of clusters “near” the DISPERSE nodes, and for clusters and their nearest DISPERSE nodes within twice the smoothing length of each other, a cluster mass-DISPERSE node density relation is seen.

DISPERSE filaments where both DISPERSE node endpoints have a matched cluster can be assigned to the corresponding cluster pair; a method for interpolating filaments through unmatched DISPERSE nodes was also applied. For smoothings $< 5 \text{ Mpc}/h$ and the “nearest/fixed/patch” methods, 10% -25% of clusters have no filament, either because they had no matching DISPERSE node (and thus did not get assigned a DISPERSE node’s filaments) or because their cluster matched DISPERSE nodes were not linked to any other cluster matched DISPERSE node. Only 47 of the clusters (out of 2898) never had a filament for any of the underlying DISPERSE webs and matching methods (152 clusters if one didn’t interpolate through unmatched DISPERSE NODES to assign filaments). Closer cluster pairs were more likely to be assigned filaments, although some of the matching methods showed a dip in this probability between 5-10 Mpc/h . Beyond 15-20 Mpc/h separations, pairs with filaments were a minority of cluster pairs (but around half of the cluster filament pairs were at larger separations). Cluster pairs with the long axis of one cluster aligned with the direction of the cluster pair also made the cluster pair more likely to be linked by a filament, and “importance” from an out of the box machine learning method also found that cluster-cluster long axis alignments made an intervening filament more likely, as expected from other studies. The average subhalo counts and mass weighted halo counts around cluster pairs are enhanced, with more enhancement for the subset of cluster pairs connected by filaments. The profile away from the filament pair was closer to $1/r$, weaker than the $1/r^2$ falloff beyond 2 Mpc/h , as found in e.g. Colberg, Krughoff & Connolly (2005); Aragon-Calvo, van de Weygaert & Jones (2010), perhaps due to assuming here that the filaments were straight lines between the pairs, but also possibly due to how filaments are defined from the underlying web. Unlike the cluster-DISPERSE node matching, where many clusters had DISPERSE node matches for most of the DISPERSE web variations and matching methods, most cluster pairs only had filaments for a few of the underlying DISPERSE web variations and matching methods.

This matching between clusters and the cosmic web picks out subclasses of both, that is, clusters and cluster pairs which have corresponding DISPERSE nodes and filaments, and vice versa. Some trends in unmatched clusters were seen, and it would be interesting to check whether others are present either in the dark matter properties or observable properties of these clusters. Unfortunately, the more recent galaxy formation models built upon the Millennium simulation are only for the rescaled (Angulo & White 2010; Angulo & Hilbert 2015) Millennium simulation, for which smooth particle densities were not available. It would be interesting to study the dif-

ferent kinds of clusters and cluster pairs which arose here in a simulation incorporating what is now known about current galaxy observables.

The unmatched DISPERSE nodes tended to be less massive but not always; those in the higher mass range, where sometimes there is a cluster match and sometimes there isn’t, would also be interesting to better understand. For example, nodes also can be evaluated in terms of other properties such as their histories (Cadiou et al 2020), just as clusters are. It also is possible to go down to lower halo (or subhalo) mass and do the matching procedure again. With more DISPERSE nodes matched to halos, the resulting network of halos (including clusters) and their inherited filaments will include more of the underlying DISPERSE web.

The clusters also give a reference point with which to compare nodes between different webs. That is, as 3/4 of the clusters had DISPERSE node matches for “nearest”, “fixed”, and “patch” matching methods and all 9 webs, the DISPERSE nodes they match to can be intercompared. This could also be done for other webs, as a way to identify corresponding nodes.

In this approach, cluster-cluster filament pairs are a particular selection of all the cluster pairs, and different underlying DISPERSE webs have different cluster pairs being assigned filaments. Unlike cluster-DISPERSE node matching, where many clusters always had matches, fewer than 10% of the cluster pairs which ever had an assigned filament had a filament for most of the different webs and matching methods; this fraction dropped by a factor of 2 if interpolation through dropped DISPERSE nodes was dropped. It would be interesting to see how much overlap there is with filaments found between clusters for other constructions which also have some sort of node-cluster identification (or have clusters defined as nodes directly).

At least for the methods of assigning filaments to cluster pairs here, whether a cluster pair shares a filament depends upon which web definition is of interest, which is a question which comes from outside of the cluster-DISPERSE node correspondence, and of course, other web finders could be used as well. One might use some of these differences between cluster filament pair properties (denser filament profile, or higher likelihood of nearby pairs being connected) as ways to characterize, and maybe select, web finders, depending upon the application in mind.

Clusters are very important gravitationally bound objects in the universe, and special environments in galaxy formation, while nodes anchor the cosmic web which evolves as structure forms. The connection between the two provides a way to better understand clusters, cosmic web nodes, and their relation and evolution together.

ACKNOWLEDGEMENTS

Many thanks especially to K. Kraljic and M. White for numerous discussions and suggestions, and to M. Alpaslan, S. Codis, C. Laigle, C. Pichon, and A. White for help as well, and to the participants of the Higgs 2019 Cosmic Web meeting, and the CCA, CERN, IAP, NYU, and the Royal Observatory of Edinburgh for hospitality and opportunities to present and discuss this work. I am also grateful to the referee, C. Miller, for many helpful questions, criticisms and suggestions,

which resulted in my making many improvements. And I am also grateful for the Millennium simulation database.

DATA AVAILABILITY

The simulation data was downloaded from the Millennium simulation database using queries which are provided in the footnotes. The cosmic webs were constructed via DISPERSE, by using the package available at <http://www2.iap.fr/users/sousbie/web/html/indexd41d.html> and then running the commands described in footnotes in the text.

REFERENCES

- Alpaslan M., et al, 2014, MNRAS, 438, 177
 Angulo R.E., White S.D.M., 2010, MNRAS, 405, 143
 Angulo R.E., Hilbert S., 2015, MNRAS, 448, 364
 Aragon-Calvo M. A., Jones B. J. T., van de Weygaert R., van der Hulst J. M., 2007, A&A, 474, 315
 Aragon-Calvo M. A., van de Weygaert R., Jones B.J.T, 2010, MNRAS, 408, 2163
 Bardeen J. M., Bond J. R., Kaiser N., Szalay A. S., 1986, ApJ, 304, 15
 Barrow J. D., Bhavsar S. P., Sonoda D. H. 1985, MNRAS, 216, 17
 Bond J.R., Kofman L., Pogosyan D., 1996, Nature, 380, 603
 Bond J.R., Myers S.T., 1996, ApJ Suppl.103, 1
 Bos E.G.P., 2016, PhD Thesis.
 Bos E.G. P., van de Weygaert R., Kitaura F., Cautun M., 2016, the Zeldovich Universe: Genesis and Growth of the Cosmic Web, Eds, R. van de Weygaert, S.F.Shandarin, E. Saar, J. Einasto, 2014 conference, arxiv: 1611.01220
 Cadiou C., Pichon C., Codis S., Musso M., Pogosyan D., Dubois Y., Cardoso J. -F., Prunet S., 2020, MNRAS, 496, 4787
 Cautun M., van de Weygaert R., Jones B. J. T., 2013, MNRAS, 429, 1286
 Cautun M. van de Weygaert R., Jones B.J.T., Frenk C.S., 2014, MNRAS, 441, 2923
 Codis S., Pichon C., Pogosyan D., 2015, MNRAS, 479, 973
 Colberg J.M., Krughoff K.S., Connolly A., 2005, MNRAS, 359, 272
 Davis, M., Efstathiou, G., Frenk, C.S., White, S.D.M., 1985, ApJ, 292, 371
 Falck B., Neyrinck M. C., 2015, MNRAS, 450, 3239
 Falck B. L., Neyrinck M. C., Szalay A. S., 2012, ApJ, 754, 12
 Fang F., Forero-Romero J., Rossi G., Li X.-D., Feng L. L., 2019, MNRAS, 485, 5276
 Forero-Romero J. E., Hoffman Y., Gottlober S., Klypin A., Yepes G., 2009, MNRAS, 396, 1815
 Hahn, O., Porciani, C., Carollo, C.M., Dekel, A., 2007, MNRAS, 375, 489
 Hahn O., Carollo C. M., Porciani C., Dekel A., 2007b, MNRAS, 381, 41
 Hellwing W.A., Cautun M., van de Weygaert R., Jones, B.T., 2021, Phys. Rev. D, 103, 063517
 “The Cosmic Web: From Galaxies to Cosmology”, 2019, Royal Observatory, Edinburgh, slides at: <https://higgs.ph.ed.ac.uk/workshops/the-cosmic-web-from-galaxies-to-cosmology/>
 Knebe, A., et al, (2011), MNRAS, 415, 2293
 Kraljic K., et al, 2019, MNRAS, 483, 3227
 Laigle C., et al, 2015, MNRAS, 446, 2744
 Leclercq F., Lavaux G., Jasche J., Wandelt B., 2016, JCAP, 08, 027
 Lemson, G., Springel, V., 2006, *Cosmological Simulations in a Relational Database: Modelling and Storing Merger Trees*, Astronomical Data Analysis Software and Systems XV, Eds., Astronomical Society of the Pacific Conference Series, 351, 212
 Libeskind N.I, et al, 2018, MNRAS, 473, 1195
 Ludlow A.D., Porciani C., 2011, MNRAS, 413, 1961
 Park D., Lee J., 2009, MNRAS, 397, 2163
 Pereyra L.A., Sgro M.A., Merchan M.E., Stasyszyn F.A., Paz D.J., 2020, MNRAS, 499, 4876
 Pfeifer, S., Libeskind, N.I., Hoffman, Y., Hellwing, W.A., Bilicki, M., Naidoo, K., 2022, arXiv:2201.04624
 Planck collaboration, Aghanim N., Akrami Y., Ashdown M., Aumont J., et al, 2020, A&A, 641, A6
 Pogosyan D., Bond J.R., Kofman L., 1998, JRASC, 92, 313
 Ramachandra N. S., Shandarin S. F., 2015, MNRAS, 452, 1643
 Rost A., Stasyszyn F., Pereyra L., Martinez H.J., 2020, MNRAS, 493, 1936
 Shandarin S., Zel’dovich Y., 1989, Rev. Mod. Phys., 61, 185
 Shandarin S. F., 2011, J. Cosmology Astropart. Phys., 5, 15
 Sousbie T., 2011, MNRAS, 414, 350
 Sousbie T., Pichon C., Kawahara H., 2011, MNRAS, 414, 0384
 Springel V., et al, 2005, Nature, 435, 629
 van de Weygaert R., Bond J.R., 2008, A Pan-Chromatic View of Clusters of Galaxies and the Large-Scale Structure, Lecture Notes in Physics, Volume 740. ISBN 978-1-4020-6940-6. Springer Science+Business Media B.V., 2008, p. 335
 van de Weygaert R., Shandarin S., Saar E., Einasto J., eds, 2016, The Zeldovich Universe: Genesis and Growth of the Cosmic Web IAU Symposium Vol. 308, doi:10.1017/S174392131601098X
 Wang P., Kang X., Libeskind N., Guo Q., Gottlober S., Wang W., 2020, New Ast. 80, 101405
 Winkel N., Pasquali A., Kraljic K., Smith R., Gallazzi A.R., Jackson T.M., 2021, arXiv:2105.1336
 Zel’dovich Y. B., 1970, A&A, 5, 84